RSC Advances

PAPER

View Article Online
View Journal | View Issue

Cite this: *RSC Adv.*, 2025, **15**, 7609

Studying on the influence of modified graphene oxide on the performance of cement-based composite materials

Yawen Gu *

In cement-based composite materials, the issue of graphene oxide (GO) dispersion has long been a bottleneck for its widespread application. In this context, polycarboxylate superplasticizer (PCS) was used to modify GO through a simple preparation process, resulting PCS@GO, which could greatly improve the dispersity of GO. It was found that PCS@GO can be uniformly dispersed in the cement mortar, a phenomenon attributed to the steric hindrance and electrostatic repulsion generated on the GO surface modified by PCS, effectively preventing the aggregation of GO. Moreover, the addition of PCS@GO significantly enhances the mechanical properties, fatigue resistance, and fluidity of the cement mortar while reducing the crystal size of the hydration products, which enhances the overall performance of the cement-based composite material. Based on the above results, this research provides theoretical support and experimental validation for the development of high-performance cement-based composite materials doped with modified GO.

Received 22nd December 2024
Accepted 27th February 2025

DOI: 10.1039/d4ra08947b

rsc.li/rsc-advances

1. Introduction

In modern society, the rapid progress in the construction field has set higher standards for the performance of building materials. As a widely used material in the construction industry, optimizing the performance of cement-based composite materials is crucial to improving the quality of buildings and extending their service life. However, these materials often face challenges such as insufficient early strength, poor crack resistance, limited bending capacity, high brittleness, slow hardening rate, and a propensity to develop micro-cracks, which can lead to structural expansion and cracking.[1–3] In recent years, the two-dimensional nanomaterial graphene oxide (GO) has been considered to have great potential in reinforcing cement-based composite materials due to its excellent physicochemical properties, such as chemical stability, ease of modification, outstanding mechanical strength, and large specific surface area.[4–10] Nonetheless, the hydrophilic functional groups on the surface of GO, such as carboxyl and hydroxyl groups, are prone to aggregate and precipitate in the high calcium and alkali environment of cement, limiting its effective application in cement-based composite materials.[11–13] To address this challenges, numerous studies have focused on improving the dispersibility of GO in cement-based composite materials, employing methods such as ultrasonic treatment, the use of dispersants, compounding with other materials, and surface modification techniques.[14–21]

Among the above strategies, surface modification technology has significant advantages over other methods, *e.g.*, without the requirement of additional stabilizers, which avoids the interface issues that might arise from introducing new components. Furthermore, surface modification strategy is also suitable for large-scale implementation, whereas ultrasonic treatment has limitations in large-scale applications. Zhao *et al.* found that introducing hydrophilic triethanolamine on the surface of GO can significantly enhance its hydrophilicity; it was demonstrated that the dispersion of triethanolamine-modified GO in cement-based composite materials is far superior to that of unmodified GO, leading to the overall performance improvement of the cement-based composite materials.[22] Remarkably, polycarboxylate superplasticizers (PCS) have been widely studied for improving the dispersion of GO in cement-based composite materials, typically used as dispersants.[23–25]

Although there are also several studies reporting the grafting of PCS onto the surface of GO, the complex preparation process and high experimental conditions required limit its feasibility in large-scale applications.[26–28] On the basis of the above discussion, it can be concluded that reducing the carboxyl group content on the surface of GO can decrease its interaction with calcium ions in cement and thus prevent aggregation, but this will also reduce the hydrophilicity of GO. Having this in mind, this study chemically bonds PCS to the surface of GO through a simple esterification reaction (*i.e.*, the reaction between the carboxyl groups on the surface of GO and the hydroxyl groups in PCS, as shown in Fig. 1), focusing on the

School of Architecture and Engineering, Lianyungang Technical College, Lianyungang 222000, China. E-mail: GYW199702@outlook.com

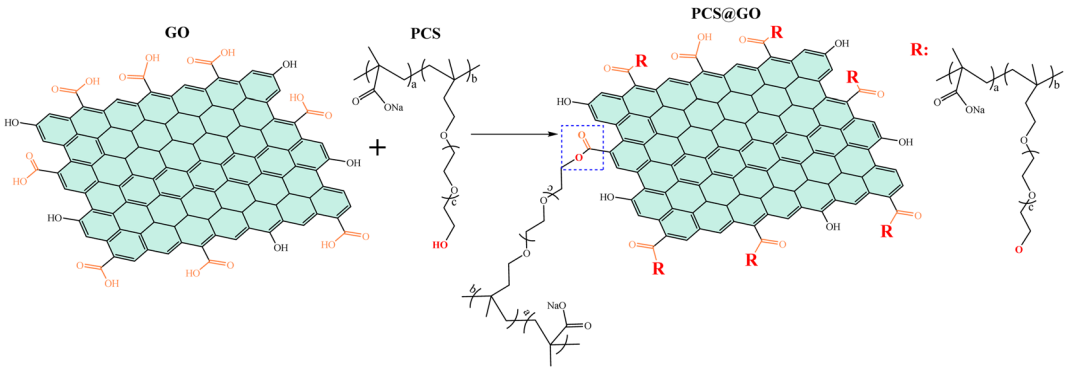

Fig. 1 Schematic diagram of PCS modified GO.

enhancement of PCS-modified GO on the performance of cement-based composite materials, including the impact on mechanical properties, fatigue performance, microstructure, and hydration rate, aiming to provide new perspective and strategy for the modification of cement-based composite materials with GO.

2. Experimental

2.1. Materials

Potassium permanganate ($KMnO_4$), graphite powder, concentrated hydrochloric acid (HCl, 37%), sodium nitrate ($NaNO_3$), concentrated sulfuric acid (H_2SO_4), calcium hydroxide ($Ca(OH)_2$), *N*,*N*-dicyclohexylcarbodiimide (DCC), and 4-dimethylaminopyridine (DMAP) were purchased from Aladdin reagent (Shanghai). Polycarboxylate superplasticizer (PCS) (structure shown in Fig. 1) was purchased from Guangzhou Chemical Reagent Factory Ltd (China) with a relative molecular mass of 26 kg mol^{-1}. Standard sand was purchased from Zhangjiakou Shifa Environmental Protection Building Materials Manufacturing Co., Ltd, with a SiO_2 content of 98.5% (mass fraction) and a fineness modulus of 2.5; P·O42.5 ordinary Portland cement was produced by Tangshan Jidong Cement Co., Ltd, and Table 1 presents the specific chemical composition of the cement.

2.2. Preparation of GO

GO was prepared according to the classic Hummers' method,[29] with the following operational details. Initially, 8.0 g of graphite powder, 10.0 g of $NaNO_3$, and 140.0 mL of concentrated H_2SO_4 were mixed in a three-necked flask, which was placed in a cooling environment at 0 °C. A magnetic stirrer was used to stir the mixture for 5 min to ensure uniform mixing of the reactants. While maintaining the reaction temperature at 0 °C, 25.0 g of $KMnO_4$ was gradually added to the flask and continuously stirred for 90 min. Subsequently, the temperature of the reaction mixture was raised to 40 °C and maintained with stirring for 2 h, after which 500.0 mL of deionized water was poured into the reaction mixture. Next, the flask was transferred to an oil bath and heated at 90 °C for 10 min. Following this, 500.0 mL of deionized water and 30.0 mL of hydrogen peroxide were added to the flask and stirring continued until no more bubbles were produced, at which point the solution turned a brownish-yellow color. The solution in the flask was then filtered while hot, and the residue was rinsed multiple times with a 5 wt% HCl solution and deionized water. Finally, the target product, GO, was obtained through freeze-drying.

Table 1 Chemical compositions of cement

	Mass weight (%)								
	CaO	SiO_2	Al_2O_3	Fe_2O_3	MgO	SO_3	K_2O	TiO_2	Na_2O
Cement	62.08	19.79	5.28	4.46	2.82	2.28	1.20	0.32	0.71

2.3. Preparation of PCS@GO

The chemical bonding of hydroxyl groups in PCS with carboxyl groups on the surface of GO was achieved through a simple DCC/DMAP catalytic esterification method.[30] The experimental procedure is briefly described as follows: First, GO was dispersed in a three-necked flask containing 6.0 mL of solvent and sonicated for 30 min to achieve uniform dispersion. Then, an appropriate amount of DCC and DMAP catalysts were added to the flask. Meanwhile, a certain quantity of PCS was dissolved in a beaker containing 4.0 mL of solvent, and after complete dissolution, this solution was slowly added dropwise to the three-necked flask containing GO and stirred at room temperature for 6 h. After the reaction was complete, the product was filtered and washed multiple times with methanol, followed by drying to obtain the PCS@GO. The dried PCS@GO was weighed and re-dispersed in deionized water for subsequent use.

2.4. Preparation of cement-based composite materials

Firstly, a predetermined amount of cement and sand were mixed with tap water and thoroughly stirred. Subsequently, PCS@GO, which was pre-dispersed in water, was added to the mixture and stirred for an additional 30 min. After that, the cement mixture containing PCS@GO was poured into a mixer, first agitated rapidly for 3 min, and then slowly for 15 min to ensure homogeneous mixing. Once uniformly mixed, the slurry was poured into molds measuring 40 mm × 40 mm × 160 mm

and cured in a standard curing chamber for 1 day, after which it was kept to continue curing for an additional 2 days (in this study, these 3 days were combined into a single curing period), as well as for further 7 days and 28 days to form the cement-based composite materials. Table 2 lists the specific composition of the cement-based composite materials, where pure Portland cement serves as the blank control group (denoted as C), the composite material doped GO is denoted as GO-C, while the composite material added PCS@GO is denoted as PCS@GO-C.

2.5. Characterizations

The X-ray diffraction (XRD) patterns of the samples were obtained using a Bruker D8 Advance diffractometer with Cu Kα radiation ($k = 1.5406°$) at 40 kV and 40 mA, scanning in the 2θ range of 5–70° at a rate of 3° min^{-1}. Fourier Transform Infrared (FT-IR) spectra were captured with an infrared spectrometer (INVENIO, Bruker, German) in the 500–4000 cm^{-1} spectral range, employing the KBr pellet technique at a resolution of 4 cm^{-1}. According to the national standard (GB/T 17671-2021), the flexural and compressive strength of the cement-based composite materials were tested using the electronic universal testing machine (HKX800) from Shanghai Hengke Instrument Technology Co., Ltd. The water absorption and fluidity of the samples were tested according to the national standard (GB/T 8077), and the setting time of the samples was tested according to the national standard (GB/T 1346). The fatigue performance of the cement-based composite materials was tested following the JT/T 860.8 testing standard using the fatigue testing machine (HS-3001A-S) from Changzhou Dedu Precision Instruments Co., Ltd.

3. Results and discussion

3.1. Structure characterizations

Fig. 2 shows the FT-IR spectra of GO and PCS@GO. As shown Fig. 2, both GO and PCS@GO exhibit a significant characteristic peak at 3300 cm^{-1}, which is attributed to the stretching vibration of O–H, indicating that a large number of hydroxyl groups still exist on the modified GO and the esterification reaction primarily occurs with the carboxyl groups of GO. In addition, the characteristic peak of the GO sample at 1720 cm^{-1} is assigned to the stretching vibration of the carboxyl groups at the edges, while in the PCS@GO sample, the absorption peak at this position noticeably shifts to a higher wavenumber (~1770 cm^{-1}) and appears as a broader peak, which is attributed to the stretching vibration of the ester groups.[31] These results indicate that the hydroxyl groups in PCS successfully

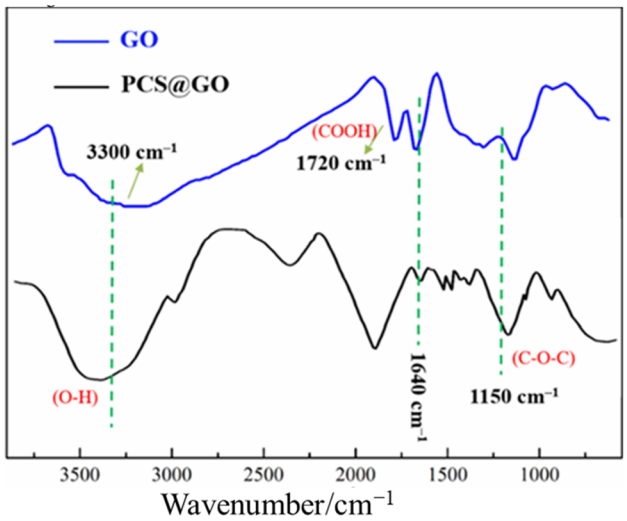

Fig. 2 FT-IR spectra of GO and PCS@GO.

react with the carboxyl groups of GO, confirming that PCS is chemically grafted onto the surface of GO rather than simply through hydrogen bonding. Additionally, the absorption peak attributed to the ether bonds of PCS structure can also be observed in the PCS@GO sample (~1150 cm^{-1}), further demonstrating the successful grafting of PCS onto the surface of GO. The peak at 1640 cm^{-1} in Fig. 2 is attributed to the characteristic signal of the double bonds in the GO structure, which can be found in both GO and PCS@GO samples, indicating that the esterification reaction did not alter the main structure of GO.[32] Clearly, the results fully illustrate that a simple esterification reaction can graft PCS onto the surface of GO.

Fig. 3 displays the XRD patterns of PCS@GO, GO, and PCS. As shown in Fig. 3, unmodified GO displays a broad hump in the 2θ range of 12–28°. This feature arises from its nano-layered structure and the disruption of graphite's original crystalline periodicity, caused by the nano-size effect.[33] When X-rays irradiate GO, the X-ray diffraction shifts to both sides, reducing the peak intensity and forming a non-sharp diffraction peak. A comparison of GO and PCS@GO reveals that the broad peak at $2\theta = 10.2°$ in GO disappears in the PCS@GO sample, which suggests that PCS macromolecules have intercalated into the GO layers, increasing the interlayer spacing and reducing van der Waals forces between them.[34] These factors contribute to the separation of GO sheets, enhancing their dispersibility. Comparing PCS and PCS@GO, it is noted that the intensity of the diffraction peaks at $2\theta = 19.3°$ and 23.2°, which could be ascribed to the polyethylene oxide side chains in the PCS macromolecules, is significantly reduced in PCS@GO,

Table 2 The compositions of cement mortars

Samples	Cement (g)	Sand (g)	Water (g)	GO (wt%)	PCS@GO (wt%)
C	550	1450	200	0	0
GO-C	550	1450	200	0.1	0
PCS@GO-C	550	1450	200	0	0.1

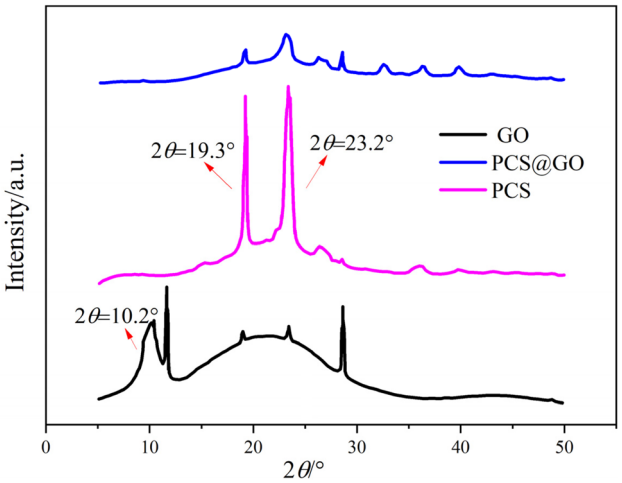

Fig. 3 XRD patterns of PCS@GO, GO and PCS.

suggesting that the grafting of PCS has altered the spatial structure of GO.[35] The steric hindrance effect of the side chains of the PCS macromolecules promotes the separation of the GO layered structure, effectively preventing the aggregation of GO in high calcium ion environments, and improving the dispersibility of GO in cement-based composite materials. The FT-IR and XRD results confirm that the PCS macromolecules have successfully grafted onto the surface and interlayers of GO, which could improve the dispersibility of GO.

Fig. 4 is a schematic illustration of the possible adsorption–dispersion of PCS@GO in cement-based composite materials based on the aforementioned characterizations. Compared to pure GO, the surface and interlayers of PCS@GO are filled with PCS macromolecules, which prevent the aggregation caused by the electrostatic interaction between the carboxyl groups on the surface of pure GO and calcium ions. The surface and interlayers of PCS@GO contain a lot of macromolecular PCS, and the steric and electrostatic repulsion between the macromolecular weights also prevent the GO sheets from coming together and aggregating. Furthermore, the macromolecular chains of PCS can also prevent calcium ions contacting with GO in an alkaline environment, further stabilizing GO. As a result, the dispersion stability of PCS@GO in cement-based composite materials could be greatly improved.

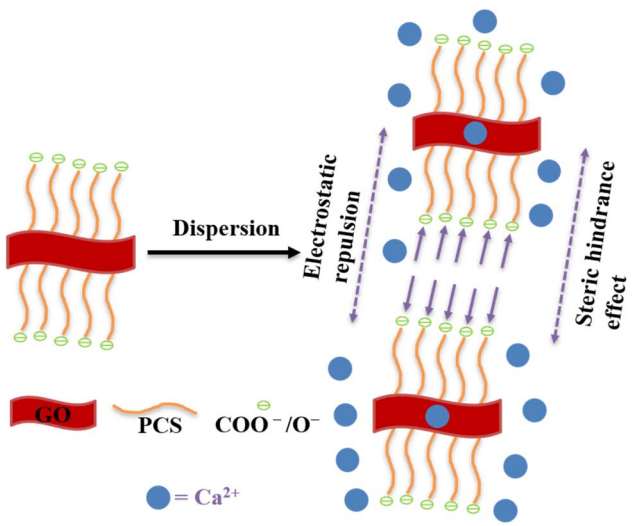

Fig. 4 Schematic diagram of the adsorption–dispersion process of PCS@GO in cement mortar.

3.2. The influence of PCS@GO on fluidity and setting time of cement-based composite materials

Table 3 summarizes the results on the fluidity, water reduction rate, and setting time of cement-based composite materials doped with PCS@GO and GO, and the blank control (C). From Table 3, it can be observed that the water reduction rate of the cement-based composite materials doped with PCS@GO significantly enhanced by 26.3%, which could be explained owing to the PCS macromolecules grafted onto GO act as an efficient water-reducing agent themselves; whereas the addition of GO decreased the water reduction rate by −6.7%, indicating the need for additional water to achieve standard fluidity. Table 3 also shows that the fluidity of the cement-based composite materials with PCS@GO (225 mm) greatly exceeded that of the samples with GO (105 mm). This is because, after adding water to the dry cement-based composite materials and stirring, a flocculated structure forms, and some water molecules become encapsulated within the paste, affecting the fluidity of the cement-based composite materials. For PCS@GO grafted by water-reducing agents, PCS@GO comes into direct contact with the paste, and its steric hindrance and electrostatic repulsion prevent the formation of the flocculated structure, reducing the encapsulated water and thereby enhancing fluidity.[36] Table 3 also reveals that the initial and final setting times of the samples with PCS@GO were increased compared to those with GO, indicating that PCS@GO has a retarding effect on the cement-based composite materials. This is because grafting hydrophilic PCS onto GO does not significantly alter its structure, promoting layer separation. As a result, the material can more easily connect with and penetrate the pores of cement-based composites, thereby delaying the setting time.

3.3. The influence of PCS@GO on the mechanical properties of cement-based composite materials

Fig. 5 shows the compressive strength (A) and flexural strength (B) of cement-based composite materials with the addition of 0.1 wt% GO, PCS@GO, and control samples at different hydration times (3 and 28 days). From Fig. 5, it can be observed that the addition of 0.1 wt% GO and PCS@GO significantly

Table 3 The water reduction rate, fluidity and setting time

Sample	Water reduction rate (%)	Fluidity (mm)	Initial setting time (min)	Final setting time (min)
C	—	130	128	185
GO-C	−6.7	105	160	235
PCS@GO-C	26.3	225	215	313

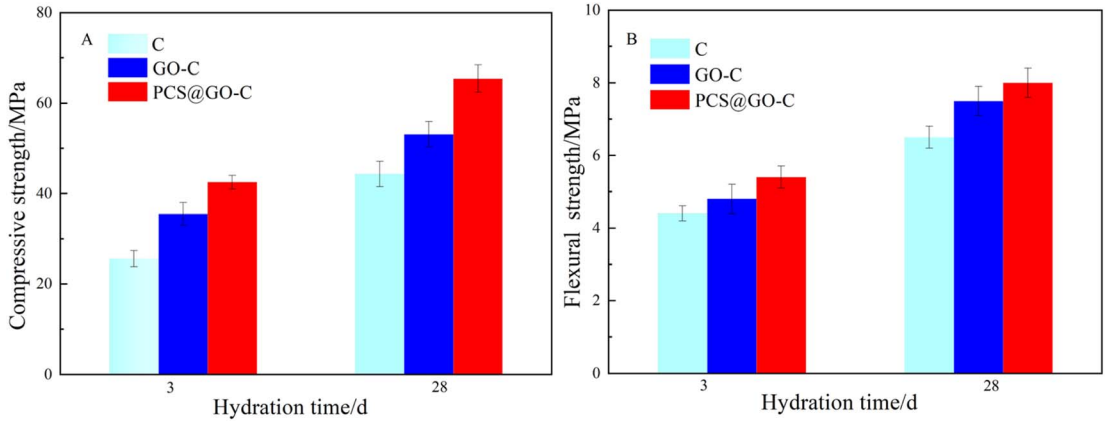

Fig. 5 The compressive strength (A) and flexural strength (B) of cement mortars that include the control, doped 0.1 wt% of GO or PCS@GO at different hydration time (3 and 28 days).

altered the compressive and flexural strengths of the cement-based composite materials. The compressive strength of the composite materials increased with hydration time (Fig. 5A), and the relationship in compressive strength is consistently PCS@GO-C > GO-C > C, indicating that the incorporation of GO is beneficial for improving the compressive strength of cement-based composite materials. Fig. 5B reveals that the flexural strength of the composite materials increased with the extension of hydration time. The flexural strength of the cement-based composite materials reached a maximum value of 8.2 MPa after 28 days, which is a 23.8% increase compared to pure Portland cement samples and a 7.3% increase compared to samples doped with 0.1 wt% GO. Similarly, when the addition of PCS@GO was 0.1 wt%, the compressive strength reached a maximum value of 65.6 MPa after 28 days, which is 47.8% higher than that of pure cement samples and 23.2% higher than cement samples doped with 0.1 wt% GO. It can be concluded that both GO and PCS@GO can improve the compressive and flexural strengths of cement-based composite materials, with PCS@GO showing a significantly higher enhancement effect than GO. It could be explained that the water-reducing effect of PCS increases the fluidity and compactness of the cement-based composite materials, reduces the void defects in the composite, and prevents stress concentration.[37] Furthermore, after grafting with PCS, the dispersibility of GO is improved, and thus PCS@GO can serve as nucleation sites for hydration crystals, which also contributes to improving the mechanical properties of cement-based composite materials.

Table 4 summarizes the fatigue resistance results of cement-based composite materials with the addition of 0.1 wt% GO, PCS@GO, and control samples at 28 days of hydration. The cement-based composite material doped with 0.1 wt% PCS@GO exhibited a fatigue life of 21.7% and 51.3% longer than that of the samples with 0.1 wt% GO and pure cement, respectively (130 με). When the strain was increased to 1000 με, the fatigue life of the sample doped with 0.1 wt% PCS@GO was 53.8% and 104.7% longer than that of the samples doped with 0.1 wt% GO and pure cement, respectively. The results suggest that the addition of PCS@GO can significantly enhance the fatigue life of cement-based composite materials, which is mainly attributed to two aspects: the bridging effect of the modified GO and the transfer of stresses from the substrate to PCS@GO itself, carrying part of the load and thus increasing fatigue resistance.[38]

Table 4 The fatigue resistance results of the samples

Samples	130 με	1000 με
C	1 122 000	6350
GO-C	1 394 500	8450
PCS@GO-C	1 698 000	13000

3.4. The influence of PCS@GO on the hydration products of cement-based composite materials

Fig. 6 exhibits the XRD patterns of C, GO-C, and PCS@GO-C samples after 3 days of hydration. It shows that the main

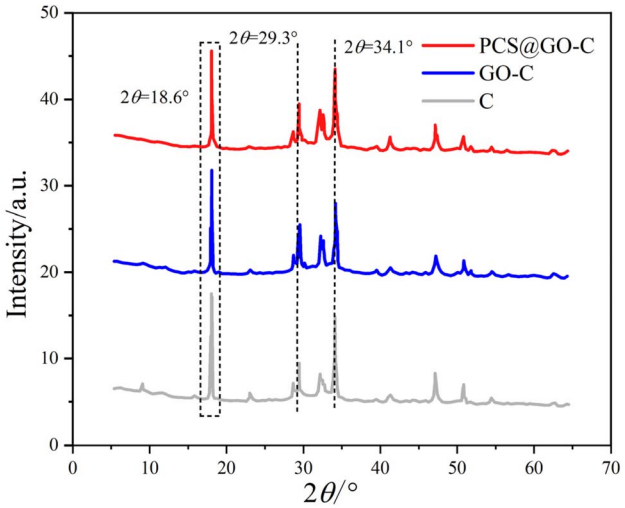

Fig. 6 XRD patterns of 3 days hydration products of cement mortar composites: C, GO-C and PCS@GO.

diffraction peaks in the XRD patterns are composed of the characteristic peaks of C_3S ($2\theta = 29.3°$), C_2S ($2\theta = 34.1°$), CH ($2\theta = 18.6°$), and ettringite ($2\theta = 8.9°$). After the addition of GO and PCS@GO, no new crystalline diffraction peaks were produced in the cement-based composite materials after 3 days of hydration. The crystalline diffraction peaks of cement clinker minerals (C_3S and C_2S) gradually weakened. The hydration product C–S–H gel, due to its poor crystallinity, appears amorphous and thus cannot be distinctly resolved in the XRD patterns. The formation of $Ca(OH)_2$ crystals is an important parameter for measuring the degree of cement hydration and the diffraction peaks at 2θ angles of 18.6°, 28.5°, 34.1°, and 47.6° in the XRD patterns confirm the presence of $Ca(OH)_2$ hydration products.[12,39]

Considering the high influence of $Ca(OH)_2$ crystals size on the mechanical properties of cement composite materials, the crystallite size was calculated by employing the Scherrer equation ($D = K\gamma/B\cos\theta$) in this work.[40] D represents the crystal size perpendicular to the diffracting plane, γ denotes the wavelength of the incident X-rays, θ is the angle of diffraction between the X-rays and the crystal plane, B is the half-height width of the diffraction peak, and K is a constant (0.89). Fig. 7 illustrates the size of CH at different crystal planes for C, GO-C, and PCS@GO-C after 3 days of hydration. It can be observed that the crystal sizes at the (001), (010), (011), and (012) planes follow the trend of C > GO > PCS@GO. The results indicate that PCS-modified GO reduced the degree of crystallization of $Ca(OH)_2$ on different crystal planes, leading to smaller crystal sizes, which is possible due to the prevention effect of PCS on the hydration of minerals in cement, thus delaying the formation of $Ca(OH)_2$ and C–S–H gels. Furthermore, the grafting of PCS onto GO increases its stability and introduces more nucleation sites, which also contributes to the reduction of crystal size. The increase in nucleation sites and the decrease in hydration product size result in a more compact curing product of the cement-based composite materials, therefore improving their mechanical properties.

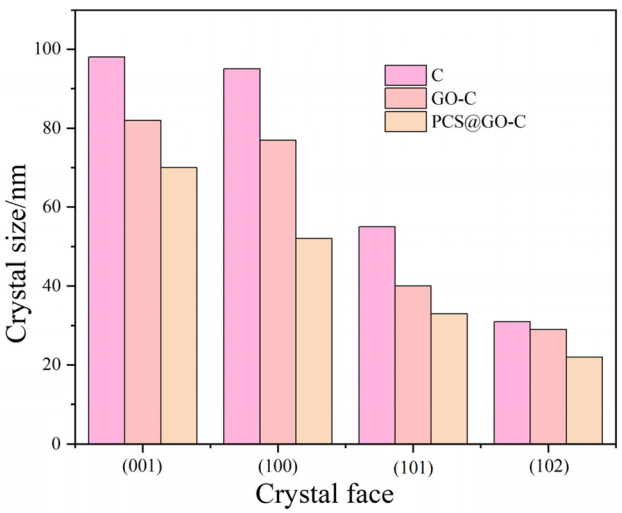

Fig. 7 The crystal size of CH products of control, doped with 0.1 wt% GO and PCS@GO at different crystal face after 3 days of hydration.

4. Conclusions

In summary, PCS@GO was successfully prepared by grafting PCS with polyethylene oxide side chains onto the surface of GO through a simple esterification reaction, and the performance of cement-based composite materials doped with PCS@GO was explored in detail. The results demonstrated that after covalent grafting of PCS, the dispersibility and fluidity of GO were significantly improved, which partially solved the aggregation problem of GO nanofillers in cement-based composite materials. Furthermore, the addition of PCS@GO can improve the compressive and flexural strengths of cement-based composite materials, and these strengths increase with the extension of hydration time. When incorporating 0.1 wt% PCS@GO, the flexural strength of the cement composite material reached a maximum value of 8.2 MPa after 28 days, which is a 23.8% improvement over pure cement samples and a 7.3% increase over sample doped with 0.1 wt% GO. Similarly, with a 0.1 wt% addition of PCS@GO, the compressive strength reached a maximum value of 65.6 MPa after 28 days, which is 47.8% higher than that of pure cement samples and a 23.2% increase over cement samples doped with 0.1 wt% GO. Furthermore, the addition of 0.1 wt% PCS@GO can significantly improve the fatigue resistance of cement-based composite materials. The XRD testing of the hydration products of PCS@GO-doped cement-based composite materials after 3 days of hydration and the size of CH crystals on different crystal planes indicate that the addition of PCS@GO reduces crystal size, making the cured composite material more compact and thus improving its performance.

Data availability

The data supporting this article have been included as part of the main text.

Author contributions

Conceptualization, resources, methodology, formal analysis, investigation, data curation, writing—original draft preparation, review and editing, visualization, supervision, validation, project administration and funding acquisition Y. W. G.

Conflicts of interest

The authors declare no conflict of interest.

Acknowledgements

The authors kindly acknowledge the financial support from Lianyungang Technical College (No. XYB202203).

References

1 M. Hasan, M. Jamil and T. Saidi, Mechanical properties and durability of ultra-high-performance concrete with calcined diatomaceous earth as cement replacement, *J. Mech. Behav. Mater.*, 2023, **32**(1), 20220262.
2 O. Zaid, N. Abdulwahid Hamah Sor, R. Martínez-García, J. de Prado-Gil, K. Mohamed Elhadi and A. M. Yosri, Sustainability evaluation, engineering properties and challenges relevant to geopolymer concrete modified with different nanomaterials: A systematic review, *Ain Shams Eng. J.*, 2024, **15**, 102373.
3 F. Sanchez and K. Sobolev, Nanotechnology in concrete – A review, *Constr. Build. Mater.*, 2010, **24**, 2060–2071.
4 S. Surehali, S. S. Volaity, A. Simon, R. Divigalpitiya, A. Kumar and N. Neithalath, New Generation Graphenes in Cement-Based Materials: Production, Property Enhancement, and Life Cycle Analysis, *ACS Sustain. Chem. Eng.*, 2024, **12**, 9193–9206.
5 Z. Liang, H. Xia, F. Yan, K. Zhang and R. Guo, The Effect of Moisture Content on the Electrical Properties of Graphene Oxide/Cementitious Composites, *Appl. Sci.*, 2024, **14**, 2819.
6 P. Verma, R. Chowdhury and A. Chakrabarti, Effect of adding highly reduced graphene oxide (rGO) nanosheets based nanomaterial on cement composites, *Mater. Today: Proc.*, 2023, DOI: **10.1016/j.matpr.2023.03.616**.
7 Y. Suo, R. Guo, H. Xia, Y. Yang, B. Zhou and Z. Zhao, A review of graphene oxide/cement composites: Performance, functionality, mechanisms, and prospects, *J. Build. Eng.*, 2022, **53**, 104502.
8 B. Han, L. Zhang, S. Zeng, S. Dong, X. Yu, R. Yang and J. Ou, Nano-core effect in nano-engineered cementitious composites, *Composites, Part A*, 2017, **95**, 100–109.
9 X. Wang, S. Dong, A. Ashour, W. Zhang and B. Han, Effect and mechanisms of nanomaterials on interface between aggregates and cement mortars, *Constr. Build. Mater.*, 2020, **240**, 117942.
10 X. Wang, S. Dong, Z. Li, B. Han and J. Ou, Nanomechanical Characteristics of Interfacial Transition Zone in Nano-Engineered Concrete, *Engineering*, 2022, **17**, 99–109.
11 X. Yao, E. Shamsaei, K. Sagoe-Crentsil and W. Duan, The interaction of graphene oxide with cement mortar: implications on reinforcing mechanisms, *J. Mater. Sci.*, 2022, **57**, 3405–3415.
12 Q. Fu, Z. Wang, Y. Xue and D. Niu, Catalysis and Regulation of Graphene Oxide on Hydration Properties and Microstructure of Cement-Based Materials, *ACS Sustain. Chem. Eng.*, 2023, **11**, 5626–5643.
13 S. Balaji and A. Swathika, Review on mechanical and microstructural properties of cementitious composites with graphene oxide, *Mater. Today: Proc.*, 2022, **50**, 2280–2287.
14 N. Asim, M. Badiei, N. A. Samsudin, M. Mohammad, H. Razali, S. Soltani and N. Amin, Application of graphene-based materials in developing sustainable infrastructure: An overview, *Composites, Part B*, 2022, **245**, 110188.
15 S. Bai, L. Jiang, N. Xu, M. Jin and S. Jiang, Enhancement of mechanical and electrical properties of graphene/cement composite due to improved dispersion of graphene by addition of silica fume, *Constr. Build. Mater.*, 2018, **164**, 433–441.
16 D. Hou, T. Yang, J. Tang and S. Li, Reactive force-field molecular dynamics study on graphene oxide reinforced cement composite: functional group de-protonation, interfacial bonding and strengthening mechanism, *Phys. Chem. Chem. Phys.*, 2018, **20**, 8773–8789.
17 A. M. Sabziparvar, E. Hosseini, V. Chiniforush and A. H. Korayem, Barriers to achieving highly dispersed graphene oxide in cementitious composites: An experimental and computational study, *Constr. Build. Mater.*, 2019, **199**, 269–278.
18 P. Zhang, M. Wang, X. Han and Y. Zheng, A review on properties of cement-based composites doped with graphene, *J. Build. Eng.*, 2023, **70**, 106367.
19 G. Xiong, Y. Ren, C. Wang, Z. Zhang, S. Zhou, C. Kuang, Y. Zhao, B. Guo and S. Hong, Effect of power ultrasound assisted mixing on graphene oxide in cement paste: Dispersion, microstructure and mechanical properties, *J. Build. Eng.*, 2023, **69**, 106321.
20 B. Han, S. Ding, J. Wang and J. Ou, *Nano-Engineered Cementitious Composites*, Springer, Singapore, 1st edn, 2019.
21 B. Han, Q. Zheng, S. Sun, S. Dong, L. Zhang, X. Yu and J. Ou, Enhancing mechanisms of multi-layer graphenes to cementitious composites, *Composites, Part A*, 2017, **101**, 143–150.
22 L. Zhao and F. Wang, Effect of amine-functionalized graphene oxide on mechanical properties of cement composites, *Inorg. Chem. Ind.*, 2023, **55**, 66–71.
23 S. Divya, S. Praveenkumar and B. A. Tayeh, Performance of modified nano carbon blended with supplementary materials in cement composite-An interpretive review, *Constr. Build. Mater.*, 2022, **346**, 128452.
24 Q. Li, C. He, H. Zhou, Z. Xie and D. Li, Effects of polycarboxylate superplasticizer-modified graphene oxide on hydration characteristics and mechanical behavior of cement, *Constr. Build. Mater.*, 2021, **272**, 121904.
25 K. Amini, A. Ghasemi, S. Soleimani Amiri, S. Mirvalad and A. Habibnejad Korayem, The synergic effects of metakaolin and polycarboxylate-ether on dispersion of graphene oxide in cementitious environments and macro-level properties of graphene oxide modified cement composites, *Constr. Build. Mater.*, 2021, **270**, 256.
26 Q. Liu, Z. Lu, X. Liang, R. Liang, Z. Li and G. Sun, High flexural strength and durability of concrete reinforced by in situ polymerization of acrylic acid and 1-acrylanmido-2-methylpropanesulfonic acid, *Constr. Build. Mater.*, 2021, **292**, 1340.
27 X. Zhang, M. Du, H. Fang, M. Shi, C. Zhang and F. Wang, Polymer-modified cement mortars: Their enhanced properties, applications, prospects, and challenges, *Constr. Build. Mater.*, 2021, **299**, 124290.
28 B. Liu, L. Wang, G. Pan and D. Li, Dispersion of graphene oxide modified polycarboxylate superplasticizer in cement

alkali solution for improving cement composites, *J. Build. Eng.*, 2022, **57**, 104860.

29 H. Guo, R. Gao, S. Liu, C. Feng, M. Qin and G. Sun, Effect of ultra-low dosage graphene oxide on the properties of recycled cement-based materials, *J. Build. Eng.*, 2024, **91**, 109637.

30 Q. Li, Y. Zhang, Z. Wu, J. Huang, N. Yue, L. Huang and X. Zhang, Tyrosine-EDC Conjugation, an Undesirable Side Effect of the EDC-Catalyzed Carboxyl Labeling Approach, *Anal. Chem.*, 2021, **93**, 697–703.

31 L. Zhao, X. Guo, C. Ge, Q. Li, L. Guo, X. Shu and J. Liu, Mechanical behavior and toughening mechanism of polycarboxylate superplasticizer modified graphene oxide reinforced cement composites, *Composites, Part B*, 2017, **113**, 308–316.

32 M. Wang and H. Yao, Comparison Study on the Adsorption Behavior of Chemically Functionalized Graphene Oxide and Graphene Oxide on Cement, *Materials*, 2020, **13**, 3274.

33 X. Yan, D. Zheng, H. Yang, H. Cui, M. Monasterio and Y. Lo, Study of optimizing graphene oxide dispersion and properties of the resulting cement mortars, *Constr. Build. Mater.*, 2020, **257**, 119477.

34 Y. Gao, J. Luo, S. Yuan, J. Zhang, S. Gao, M. Zhu, Z. Li and X. Zhou, Fabrication of graphene oxide/fiber reinforced polymer cement mortar with remarkable repair and bonding properties, *J. Mater. Res. Technol.*, 2023, **24**, 9413–9433.

35 X. Zhang, S. Zhou, H. Zhou and D. Li, The effect of the modification of graphene oxide with γ-aminopropyltriethoxysilane (KH550) on the properties and hydration of cement, *Constr. Build. Mater.*, 2022, **322**, 126497.

36 Y. Zhao, J. Zhang, G. Qiao, D. Hou, B. Dong and H. Ma, Enhancement of Cement Paste with Carboxylated Carbon Nanotubes and Poly(vinyl alcohol), *ACS Appl. Nano Mater.*, 2022, **5**, 6877–6889.

37 L. Wu, S. Lv, Z. Li, Y. Li and L. Liu, Dispersion Behavior of Ultra-low Dosage Graphene Oxide and its Effect on Structures and Performances of Cement-Based Materials, *Acta Mater. Compositae Sin.*, 2023, **40**, 2296.

38 W. Zhao, Y. Chen, Z. Liu, L. Wang and X. Li, Effects of surface-modified coal-bearing metakaolin and graphene oxide on the properties of cement mortar, *Constr. Build. Mater.*, 2023, **372**, 130796.

39 S. Lv, L. Wu, Z. Li, R. Gao and L. Liu, Investigation of dispersion behavior of GO in aqueous and effect of ultra-low dosage GO on structure and properties of cement-based composites, *Constr. Build. Mater.*, 2022, **350**, 128828.

40 U. Holzwarth and N. Gibson, The Scherrer equation versus the 'Debye-Scherrer equation', *Nat. Nanotechnol.*, 2011, **6**, 534.